APL Materials

Growth of non-polar (11-20) InGaN quantum dots by metal organic vapour phase epitaxy using a two temperature method

Cite as: APL Mater. **2**, 126101 (2014); https://doi.org/10.1063/1.4904068
Submitted: 25 September 2014 . Accepted: 01 December 2014 . Published Online: 12 December 2014

J. T. Griffiths, T. Zhu, F. Oehler, R. M. Emery, W. Y. Fu, B. P. L. Reid, R. A. Taylor, M. J. Kappers, C. J. Humphreys, and R. A. Oliver

openaccess

View Online Export Citation CrossMark

ARTICLES YOU MAY BE INTERESTED IN

Non-polar (11-20) InGaN quantum dots with short exciton lifetimes grown by metal-organic vapor phase epitaxy
Applied Physics Letters **102**, 251905 (2013); https://doi.org/10.1063/1.4812345

Improvement of single photon emission from InGaN QDs embedded in porous micropillars
Applied Physics Letters **113**, 101107 (2018); https://doi.org/10.1063/1.5045843

Spectral diffusion time scales in InGaN/GaN quantum dots
Applied Physics Letters **114**, 112109 (2019); https://doi.org/10.1063/1.5088205

AMERICAN ELEMENTS
THE ADVANCED MATERIALS MANUFACTURER®
The Next Generation of Material Science Catalogs
Now Invent.™
www.americanelements.com
© 2001-2021 American Elements is a U.S Registered Trademark

© 2014 Author(s).

AIP Publishing

Growth of non-polar (11-20) InGaN quantum dots by metal organic vapour phase epitaxy using a two temperature method

J. T. Griffiths,[1] T. Zhu,[1] F. Oehler,[1] R. M. Emery,[1] W. Y. Fu,[1] B. P. L. Reid,[2] R. A. Taylor,[2] M. J. Kappers,[1] C. J. Humphreys,[1] and R. A. Oliver[1]
[1]*Department of Materials Science and Metallurgy, University of Cambridge, Cambridge CB3 0FS, United Kingdom*
[2]*Department of Physics, University of Oxford, Oxford OX1 3PU, United Kingdom*

(Received 25 September 2014; accepted 1 December 2014; published online 12 December 2014)

Non-polar (11-20) InGaN quantum dots (QDs) were grown by metal organic vapour phase epitaxy. An InGaN epilayer was grown and subjected to a temperature ramp in a nitrogen and ammonia environment before the growth of the GaN capping layer. Uncapped structures with and without the temperature ramp were grown for reference and imaged by atomic force microscopy. Micro-photoluminescence studies reveal the presence of resolution limited peaks with a linewidth of less than ~500 μeV at 4.2 K. This linewidth is significantly narrower than that of non-polar InGaN quantum dots grown by alternate methods and may be indicative of reduced spectral diffusion. Time resolved photoluminescence studies reveal a mono-exponential exciton decay with a lifetime of 533 ps at 2.70 eV. The excitonic lifetime is more than an order of magnitude shorter than that for previously studied polar quantum dots and suggests the suppression of the internal electric field. Cathodoluminescence studies show the spatial distribution of the quantum dots and resolution limited spectral peaks at 18 K. © *2014 Author(s). All article content, except where otherwise noted, is licensed under a Creative Commons Attribution 3.0 Unported License.* [http://dx.doi.org/10.1063/1.4904068]

Quantum dots (QDs) offer the potential to confine carriers in all three spatial dimensions due to their quasi-zero-dimensional nature, which results in a delta-function-like density of states and discrete energy levels. This atom-like nature has been shown to lead to photon anti-bunching[1] and hence single photon emission. QDs have, therefore, been proposed as viable structures as building blocks for quantum logic gates,[2,3] as well as for applications in quantum cryptography.[4]

Nitride based QDs are of particular interest since the emission wavelength may theoretically be controlled over the UV to IR spectrum through variations in the group III alloy content. The large band offsets between the QD and the matrix material combined with the large exciton binding energy have been shown to lead to single photon emission up to room temperature.[5]

However, nitride QDs are most commonly grown on the basal plane, which contains an inherent electric field directed along the polar axis. The internal electric field results in the spatial separation of the electron and hole wavefunctions, which leads to longer exciton lifetimes. The presence of the internal electric field may also be responsible for the variation in the emission wavelength and linewidth over time (spectral diffusion).[6] Theoretical work has suggested that growth in the non-polar orientations may eliminate the in-plane electric field.[7] Previous work by Zhu *et al.*[8] has demonstrated the growth of non-polar *a*-plane InGaN QDs by the modified droplet epitaxy (MDE) method with exciton lifetimes an order of magnitude smaller than comparable polar QDs,[9] and which exhibit improved temperature stability[10] and Rabi oscillations.[11] However, the photoluminescence (PL) linewidth of the QDs grown by MDE remains typically in excess of 1 meV. It is not clear whether this is a measure of the true linewidth of the emission, or whether the measurement is affected by spectral diffusion.

 © Author(s) 2014

In this letter, an alternative method for the growth of non-polar (11-20) InGaN QDs by metal organic vapour phase epitaxy (MOVPE) is reported, utilising a temperature ramp in an ammonia and nitrogen environment to achieve improved luminescence properties. Low temperature cathodoluminescence (CL) and micro-photoluminescence (μPL) show the presence of sharp peaks in the collected spectra, whose linewidth is limited by the resolution of the detection system. Time resolved PL studies have been used to measure the lifetimes to give an insight into the internal electric field.

The samples were grown in a 6×2 in. Thomas Swan close-coupled showerhead reactor by MOVPE on *r*-plane (1-102) sapphire substrates. Trimethylgallium, trimethylindium, and ammonia were used as the precursors. The growth temperatures cited here are those of the SiC-coated graphite susceptor below the substrate measured by emissivity-corrected pyrometry (EpiTT by Laytec AG). GaN *a*-plane pseudo-substrates were prepared by a silicon nitride interlayer (SiN_x) technique to reduce the dislocation density.[12]

A low-temperature nucleation layer was grown, followed by a two-dimensional (2D) growth step and the deposition of a SiN_x interlayer for 600 s using a SiH_4 flux of 200 nmol/min and an ammonia flow of 446 mmol/min. A short period of three-dimensional growth at a V/III ratio of 1900 was then carried out to form islands, which was followed by coalescence and 2D growth at a V/III ratio of 60 and then by a further ~500 nm GaN growth at a V/III ratio of 740 to improve the luminescence properties. The final threading dislocation density was approximately 3×10^9 cm^{-2} and the basal plane stacking fault (BSF) density approximately 5×10^5 cm^{-1}.[13]

An InGaN epitaxial layer (~16 ML) was grown at 680 °C and 300 Torr and subjected to a temperature ramp over 90 s to 860 °C in a mixture of nitrogen and ammonia, which was followed by the growth of a 10 nm GaN cap layer at 860 °C, and another 10 nm GaN cap at 1050 °C at 100 Torr in hydrogen. Uncapped epilayer structures were also grown to study the effect of the temperature ramp on the surface morphology of the InGaN. To reproduce the effect of the temperature ramp on the surface morphology of the InGaN, an InGaN epilayer was subjected to a temperature ramp up to 860 °C, and then immediately cooled to room temperature; we refer to such samples as "temperature bounced (T-bounced)." For comparison, another InGaN epilayer was grown and cooled immediately from the InGaN growth temperature to room temperature, without a temperature bounce.

Atomic force microscopy (AFM) was performed on a Veeco Dimension 3100 with RTESP tips from Bruker-Nano with a nominal radius of 8 nm in tapping mode. A Gatan MonoCL4 system was used to study to the CL signal in a Phillips XL30s field emission scanning electron microscope (SEM) operated at 4 keV equipped with a liquid helium cold stage.

Two-photon excitation μPL measurements were performed on a cold-finger cryostat stage cooled to 4.2 K. The excitation source was a 1 ps duration, mode-locked Ti:Sapphire laser emitting at 1.55 eV, with a spectral linewidth of 1.3 meV. The excitation laser pulses were focussed with an objective lens to a spot size of ~1 μm with an excitation power density of 1 MW cm^{-2}. The PL signal was focussed onto a 50 μm entrance slit before being dispersed by a 1200 l/mm grating in a 0.3 m spectrometer and detected on a Si-based charge-coupled device (CCD). Time resolved PL measurements were also performed at 4.2 K using a time-correlated single photon counting system with a time resolution of 130 ps. Electron beam lithography was used to produce an Al mask on the sample with 1 μm aperture sizes and alignment markers as detailed in Ref. 14.

AFM imaging of the surface of the uncapped T-bounced epilayer shown in Figure 1(a) reveals the presence of nanostructures distributed uniformly across the structure with a mean density of $(7.7 \pm 0.4) \times 10^7$ cm^{-2} with a mean height of 10.7 nm and standard deviation of 1.6 nm. AFM imaging of the uncapped T-bounced epilayer after a treatment at room temperature with a HCl/H_2O (1:3) solution suggests that the nanostructures are resistant to the etching. It is therefore believed that the nanostructures are not metallic droplets, unlike those observed following an anneal treatment in N_2 in the MDE technique,[8] but consist of crystalline InGaN.

To investigate the nature of the growth mechanism, the uncapped sample grown without a temperature bounce step was imaged by AFM, as shown in Figure 1(b). In this case, there is a significantly higher density of nanostructures $(1.5 \pm 0.1) \times 10^{10}$ cm^{-2}. The nanostructures on the sample without a T-bounce are significantly larger, with a mean height of 17.2 nm with a standard deviation of 6.3 nm.

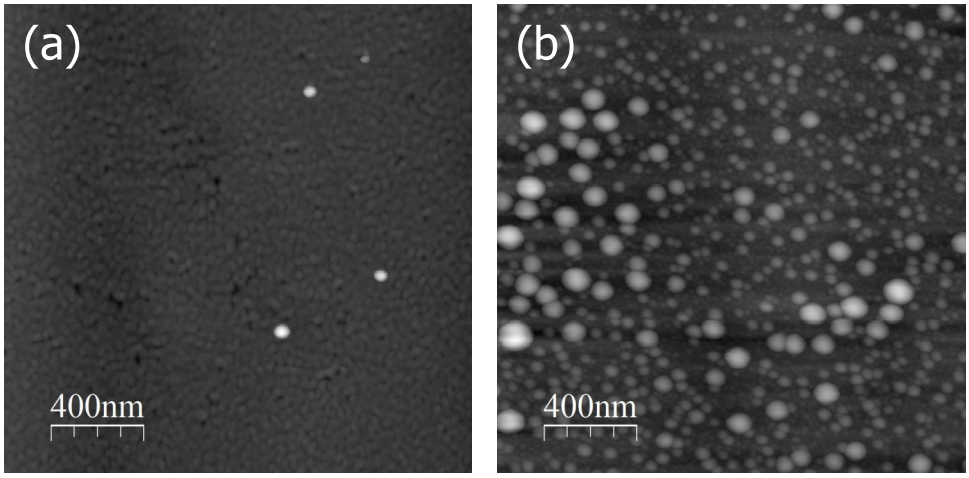

FIG. 1. AFM images InGaN epilayers grown (a) with the T-bounce (height 31 nm) and (b) without the T-bounced growth (height 62 nm).

In PL measurements of the epilayer grown without the T-bounce procedure, we have not observed any luminescence at room temperature unlike the T-bounced sample, which exhibits room temperature luminescence with a peak at 480 nm. We therefore suggest that at least the largest of the nanostructures observed in AFM may be relaxed through the formation of misfit dislocations or other defects. The defects serve as deeper non-radiative centres which quench the emission, possibly also from the surrounding defect free nanostructures. We propose that the temperature ramp leads to desorption of the relaxed structures, which are likely to be more In-rich. Smaller, lower In content epitaxially strained structures remain after the desorption. We suggest that the nanostructures observed prior to the temperature ramp might have formed by Stranski-Krastanov growth or a variant, and that it may be possible to grow luminescent nanostructures without the temperature ramp, by reducing the build-up of strain energy in the InGaN layer. This might be achieved either by increasing the InGaN growth temperature and hence lowering the In content or by reducing the layer thickness, and these approaches are under investigation.

Figure 2 shows a μPL spectrum from the capped sample grown using a temperature ramp. The data come from a 1 μm diameter window in a masked region to limit the illuminated area and improve the spatial resolution. The spectrum was collected at 4.2 K and shows narrow peaks limited by the resolution of the system (~500 μeV) which indicates the presence of excitons confined within QDs. The observed narrower linewidth (<500 μeV) compared to the QDs grown by the MDE technique (~1 meV) may be indicative of a reduced spectral diffusion, and therefore may

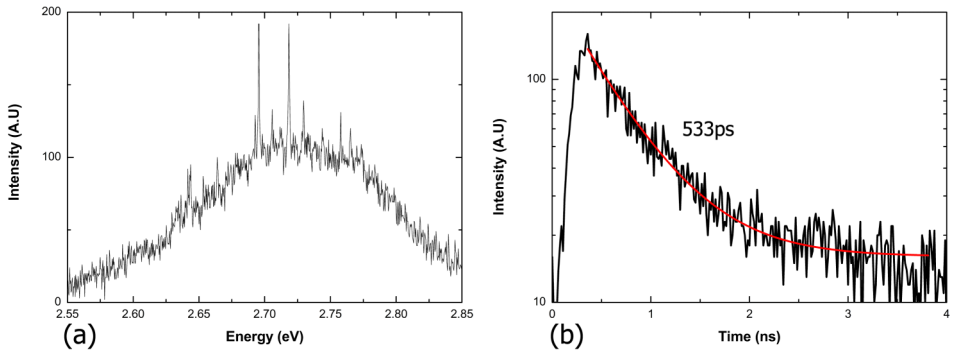

FIG. 2. (a) μ-PL spectrum obtained over a 1 μm masked region with spot size 1 μm at 4.2 K. (b) μPL decay spectrum at an emission energy of 2.70 eV, performed at 4.2 K.

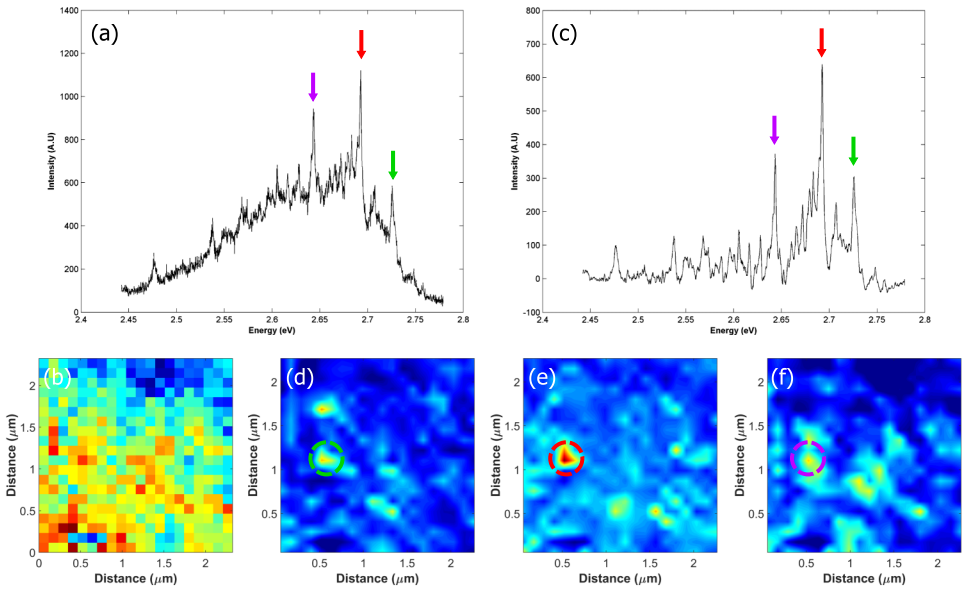

FIG. 3. CL spectra recorded at 4 keV at 18 K (a) raw extracted spectrum, (b) raw spectral image, (c) extracted spectrum with the Gaussian background removed. Extracted and Gaussian background subtracted monochromatic CL images at emission energies (d) 2.72 eV, (e) 2.68 eV, and (f) 2.63 eV from the same area.

represent an advantage of this growth method. However, the PL spectrum shown in Figure 2 exhibits a strong background emission underlying the QD peaks, which is believed to be related to the quantum well-like InGaN wetting layer underlying the QDs. The strong background may be a potential disadvantage in the development of single photon sources since emission from other structures may contaminate the single photon emission from the QD unless suppressed.

Time correlated single photon counting was performed to measure the excitonic lifetime and to study the effect of the internal electric field on the electron and hole wavefunctions. A monoexponential decay was observed for the sharp peak at 2.70 eV, shown in Figure 2(b), with a lifetime of 533 ps. The lifetime is comparable to the QDs grown by the MDE method but significantly shorter than polar structures. QDs grown on the *c*-plane with emission energy of 2.86 eV and 2.82 eV have shown lifetimes in excess of 60 ns (Ref. 9) and 20 ns (Ref. 15), respectively. The short lifetime suggests a stronger overlap of the electron and hole wavefunction and the suppression of the internal electric field relative to polar QDs.

CL spectrum imaging of the capped T-bounced structure was performed at 18 K, over an area of 2.32 μm by 2.32 μm with a pixel size of 116 nm. Each pixel corresponds to a CL spectrum with a spectral resolution of ~2 meV, recorded by a CCD. Figure 3(a) shows the CL spectrum corresponding to the pixel identified in the raw spectrum image of Figure 3(b). The spectrum shows the presence of three resolution limited peaks identified by arrows in Figure 3(b), superimposed upon a broad background centred at 2.64 eV.

The intensity in the spectrum image of Figure 3(b) is dominated by the broad emission from the underlying wetting layer. To enhance the CL intensity of the QDs, the background was modelled as a Gaussian function and subtracted from the spectrum of each pixel. Figure 3(c) shows the CL spectrum corresponding to the identified pixel with the Gaussian background subtracted. Using the background subtracted data, monochromatic CL images were extracted at the energies corresponding to the resolution limited peaks identified in the spectrum, as shown in Figures 3(d)–3(f). Dashed circles indicate the position of the extracted spectrum on the monochromatic images. The images were linearly interpolated. Monochromatic images show the spatial distribution of the intense luminescent features from which resolution limited peaks are observed revealing a spatial density of $(9.3 \pm 1.8) \times 10^7$ cm^{-2} which is comparable to the density of nanostructures observed by AFM within the stated errors, suggesting that the bright luminescence features relate to the structures seen

in AFM. The direct correlation between the density of nanostructures and the number of resolution limited spectral features suggests that the origin of the resolution limited peaks is from the QDs and not from localisation centres in the underlying wetting layer. Spectrum imaging suggests that a number of resolution limited peaks are present within each high intensity position, which suggests that each high intensity region may contain either one QD exhibiting a number of spectrally distinct transitions or more than one QD.

In conclusion, non-polar (11-20) InGaN QDs grown by MOVPE using a two temperature method have been demonstrated. Both CL and μPL measurements have shown resolution limited peak linewidths at 18 K and 4.2 K, respectively, confirming the formation of QDs. The observed narrower linewidth compared to the QDs grown by the MDE technique may represent an advantage of this novel technique in the advancement of single photon sources. A strong luminescent background is observed that may aid in the performance of lasers however, may be detrimental to the development of single photon sources. Exciton lifetimes an order of magnitude shorter than equivalent polar structures have been observed suggesting the suppression of the electric field and stronger confinement of the wavefunctions.

This work was funded by the EPSRC (Grant Nos. EP/J003603/1 and EP/H047816/1).

[1] H. Kimble, M. Dagenais, and L. Mandel, Phys. Rev. Lett. **39**, 691 (1977).
[2] D. Loss and D. P. DiVincenzo, Phys. Rev. A: At., Mol., Opt. Phys. **57**, 120 (1998).
[3] S. De Rinaldis, I. D'Amico, E. Biolatti, R. Rinaldi, R. Cingolani, and F. Rossi, Phys. Rev. B: Condens. Matter Mater. Phys. **65**, 081309(R) (2002).
[4] S. Wiesner, ACM SIGACT News **15**, 78 (1983).
[5] M. Holmes, K. Choi, S. Kako, M. Arita, and Y. Arakawa, Nano Lett. **14**, 982 (2014).
[6] I. A. Ostapenko, G. Honig, C. Kindel, S. Rodt, A. Strittmatter, A. Hoffmann, and D. Bimberg, Appl. Phys. Lett. **97**, 063103 (2010).
[7] A. E. Romanov, T. J. Baker, S. Nakamura, and J. S. Speck, J. Appl. Phys. **100**, 023522 (2006).
[8] T. Zhu, F. Oehler, B. P. L. Reid, R. M. Emery, R. A. Taylor, M. J. Kappers, and R. A. Oliver, Appl. Phys. Lett. **102**, 251905 (2013).
[9] R. A. Oliver, A. Jarjour, R. A. Taylor, A. Tahraoui, Y. Zhang, M. J. Kappers, and C. J. Humphreys, Mater. Sci. Eng. B **147**, 108 (2008).
[10] B. P. L. Reid, T. Zhu, C. C. S. Chan, C. Kocher, F. Oehler, R. Emery, M. J. Kappers, R. A. Oliver, and R. A. Taylor, Phys. Status Solidi C **11**, 702 (2014).
[11] B. P. L. Reid, C. Kocher, T. Zhu, F. Oehler, R. M. Emery, C. C. S. Chan, R. A. Oliver, and R. A. Taylor, Appl. Phys. Lett. **104**, 263108 (2014).
[12] C. F. Johnston, M. J. Kappers, M. A. Moram, J. L. Hollander, and C. J. Humphreys, J. Cryst. Growth **311**, 3295 (2009).
[13] R. Hao, M. J. Kappers, M. A. Moram, and C. J. Humphreys, J. Cryst. Growth **337**, 81 (2011).
[14] B. P. L. Reid, T. Zhu, T. J. Puchtler, L. J. Fletcher, C. C. S. Chan, R. A. Oliver, and R. A. Taylor, Jpn. J. Appl. Phys., Part 1 **52**, 08JE01 (2013).
[15] R. A. Oliver, G. Andrew, D. Briggs, M. J. Kappers, C. J. Humphreys, S. Yasin, J. Rice, J. Smith, and R. A. Taylor, Appl. Phys. Lett. **83**, 755 (2003).